Traction Calculations and Design Data for Two Traction Fluids*

Joseph Leo Tevaarwerk†

Traction drives for automotive applications have a rather checkered history. After a brief period of acceptance during the first quarter of this century they disappeared in rapid fashion. The main reason for their initial acceptance was the simplicity with which a variable speed output can be obtained from a nearly constant input speed. Their rapid demise was due to the fact that, while simple in concept, the average life expectancy was very low indeed. With the advent of a more demanding motoring public, this short life expectancy became unacceptable, and other solutions were found to the speed match problem. In recent years traction drives have had a resurgence because of the energy crisis and the fact that a lot of the initial problems have now been, partially, at least, solved.

In simple terms the basic elements in a traction drive are two rollers, pressed into nominal contact and rolled about their respective axes. Power is transmitted in the form of a shear stress across the contact area. A fluid is present to prevent initial surface scuffing damage and to provide for some form of cooling. The rolling motion of the disks draws this fluid into the contact zone, and a thin layer of this fluid will separate the actual contact area. It is also in this region where the torque is transmitted from one roller to the next, and it should not surprise one that the performance of a traction drive depends to a large extent upon the rheological properties of the fluid. Close examination of the fluid as it passes through the contact gap reveals that it experiences a sudden pressure pulse from atmospheric to possibly several gigapascals in a period of 1 to 0.1 msec. The shear stress that is transmitted from one disk to the other (about 10 percent of the normal stress) passes through this layer of fluid "trapped" in the contact and causes a shear. This, in turn, will lead to heat generation, and from simple calculations, temperatures in the center of the film can easily reach several hundred degrees centigrade.

To study the rheological properties of the fluid under these conditions precludes the use of most of the conventional instruments used for steady-state measurement. In fact the only suitable type of instrument is a disk machine where most of the conditions are the same or similar to those in traction drives. From the resulting traction tests, certain models are inferred, and it is in this area where there has been a lot of activity recently.

To the designer of traction drives, the traction behavior of the fluid under the severe conditions is of utmost importance because of the direct influence that it has on the efficiency, size, and life of a given drive.

Previous Traction Investigations

As mentioned in the introduction, there has been a lot of activity in the area of traction research, both in the past and recently. Notable contributions have come from Clark, et al., Hewko, Smith, Smith, et al., Johnson and Cameron, Niemann, and more recently Johnson and Roberts and Johnson and Tevaarwerk (refs. 1 to 8). Some of these investigations were strictly experimental, and aimed at obtaining traction-drive design data, while others were aimed at understanding the traction phenomena so that rheological models could be formulated. This latter research is, of course, ultimately aimed at relating fluid molecular properties to traction properties. Research by Johnson and Tevaarwerk (ref. 8), Daniels (ref. 9), Hirst and Moore (ref. 10), and Alsaad, et al. (ref. 11) is directed specifically towards this purpose. The reader is referred to an excellent review by Johnson (ref. 12) for further aspects of this topic.

*Work done under contract DEN 3-35.
†Applied Tribology, Ltd.

Many of the rheological models derived so far have been isothermal because of the degree of complexity that thermal analysis introduces. Thermal effects are important. However, a simple method is sought to include them in the analysis.

Current understanding of traction has led to traction models that describe the fluid shear behavior in terms of an elastic and a dissipative element. An analysis of traction-drive performance using such a model was done by Tevaarwerk (ref. 13). It showed that under certain conditions the prediction technique by Magi (ref. 14) can be used. The work of reference 13 has recently been further expanded by developing a simple method to correct for thermal effects due to spin (ref. 15) and by performing an overall thermal traction study (ref. 16).

As with all models, however, their usefulness is severely restricted if inadequate input traction data are available to the designer. This is especially so if high-traction fluids are used that have not been tested extensively for use under the wide range of conditions that exist in modern, highly advanced traction drives.

Nomenclature

		First used
A_i	regression constants	eq. (11)
a,b	semi-Hertz contact size for x,y direction, m	eq. (1)
C_i	regression constants for traction variables	eq. (14)
F_x	contact force in the x-direction, N	eq. (5)
F_z	normal force on the contact, N	eq. (5)
$\overline{G}$	average fluid shear modulus for contact, Pa	eq. (1)
h	EHL film thickness of the fluid in contact, m	eq. (1)
J_1	dimensionless longitudinal slip variable	eq. (4)
J_2	dimensionless side slip variable	eq. (9)
J_3	dimensionless spin variable	eq. (6)
J_4	dimensionless traction variable	eq. (5)
k	contact aspect ratio, $=b/a$	eq. (4)
$k_{1,2}$	coefficients for rigid/plastic model	eq. (8)
m	initial slope for zero spin traction curve	eq. (1)
p	Hertzian contact pressure, GPa	eq. (11)
S	dimensionless slip grouping	eq. (9)
U	rolling speed of the disks, m/sec	eq. (4)
ΔU	longitudinal slip velocity of the disks, m/sec	eq. (4)
ΔV	side slip velocity of the disks, m/sec	eq. (9)
Z	dimensionless spin grouping	eq. (15)
ϵ	speed pole parameter	eq. (7)
θ	temperature of the inlet fluid, °C	eq. (11)
μ	peak traction coefficient for a given test	eq. (2)
$\overline{\tau}_c$	critical shear strength of fluid, Pa	eq. (2)
ω	spin velocity on the contact, rad/sec	eq. (6)
Superscripts		
$'$	nondimensional regression variable	
$\overline{\ }$	denotes averaged variables	

Traction Predictions

The principal traction information for the designer comes from the so-called traction curve. This curve is obtained by sliding and rolling two disks relative to each other and measuring the resulting

traction force. The data are normally plotted in dimensionless form as traction coefficient versus slide to roll ratio. Figure 1 shows such a typical curve. The exact shape and features of this curve depend on several external variables such as type of fluid, contact pressure, rolling speed, inlet temperature, and the kinematic conditions that exist in the contact. These kinematic conditions may consist of spin, side slip, and longitudinal slip, or a combination of these. It is, of course, not practical to experimentally measure the traction under every single variation of these conditions, so traction models are resorted to. With a suitable traction model and the knowledge of a few of the fluid rheological parameters, traction under varying kinematic conditions can then be predicted. Present-day traction models take into account the fluid and disk elasticity effect as well as the dissipative behavior of the fluid film. This model can be simplified for purposes of traction-drive analysis to a simple linear elastic spring in series with a Coulomb friction model (fig. 2).

The method of operation of this model is as follows: Upon the application of a shear force, τ, the linear spring element will extend. This extension is directly proportional to the stress at all levels of stress until a certain critical stress τ_c is reached. At this point the Coulomb friction is insufficient, and the extension in the spring element ceases. Sliding will now take place provided that the stress is maintained at τ_c. Upon a reduction or reversal of stress, the elastic element will retract and recover the energy stored in it. The frictional work is, however, lost. (This frictional work will result in heat generation which, in turn, results in a local temperature rise. This temperature rise influences the level of stress, τ_c, in a complicated manner but always reduces it.) The modulus, G, of the elastic element is related to the initial traction slope through contact geometry and the kinematic conditions.

For simple slip traction curves, m and G are related as follows:

$$\bar{G} = \frac{3}{8} m F_z \frac{\bar{h}}{a^2 b} \tag{1}$$

where $\bar{h}$ is the average film thickness, a and b are the semicontact dimension, and F_z is the contact normal load. The quantity $\bar{G}$ is indicated here rather than G. This is to signify that we only deduce an average shear modulus. The reason for this is that we do not know exactly how the fluid shear modulus is influenced by the local pressure in the contact. (The extraction of G for the fluid is further

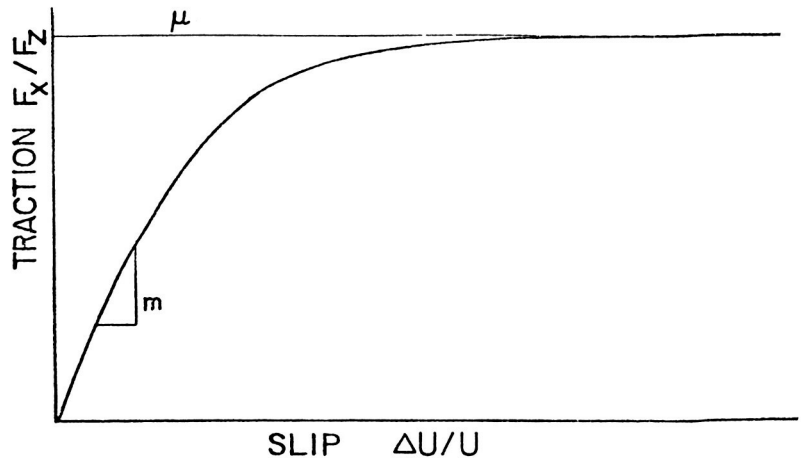

Figure 1. - General features of a traction curve showing the initial traction slope m and the peak traction coefficient μ.

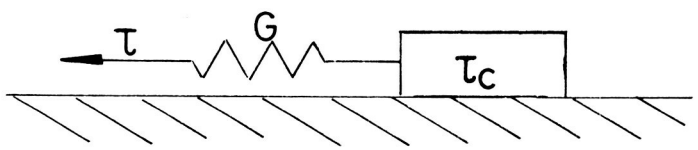

Figure 2. - Schematic of the elastic/plastic traction model.

complicated by the fact that in the traction slope a certain amount of elastic creep of the disk material is invariably present.)

The frictional stress, τ_c, is directly related to the peak traction coefficient, μ, through the following equation:

$$\bar{\tau}_c = \mu \frac{F_z}{\pi ab} \tag{2}$$

Again, we are only extracting the average quantity τ_c because of the lack of knowledge about the variation of τ_c with pressure. (This limiting stress is temperature dependent. The temperature of the fluid is not constant but rises as more and more slip occurs on the contact. For simplicity, however, we often use the peak traction coefficient, if such a peak exists.) A detailed description of how this model can be used to predict traction under conditions of spin, side slip, and the usual longitudinal slip is given by Tevaarwerk and Johnson (ref. 17) and Tevaarwerk (ref. 13). The analysis described in these references is entirely isothermal in nature.

To show how powerful this model is, consider the traction curves shown in figure 3 and reported by Tevaarwerk (ref. 18). These are curves obtained under a variety of conditions on two different traction testers and with two different fluids. Yet, by using an elastic/plastic traction model, all these curves can be reduced to fall on a single master traction curve (fig. 4). Each individual traction curve requires now only two parameters to describe it completely: the initial slope, m, and the peak traction coefficient, μ. This applies only to the simple slip traction curves, but the important parameters, m and μ, can be used to predict traction under any combination of spin and slip.

Theoretical Traction Results

The theoretical traction results, as calculated by Tevaarwerk and Johnson (ref. 17) and Tevaarwerk (ref. 13), for the elastic/plastic model are now presented. The reader is referred to the above two papers for further details. Although for a number of special cases analytical solutions exist, the general situation of combined slip, side slip, and spin was solved using digital techniques.

Traction Due to Slip

For simple dimensionless slip, J_1, on the contact aspect ratio, k, the resulting traction, J_4, is as follows:

$$J_4 = \frac{1}{\pi}\left[2 \tan^{-1} S + \frac{2S}{1+S^2}\right] \tag{3}$$

where $S = \frac{2}{3}\frac{J_1}{\sqrt{k}}$

and the dimensionless slip is

$$J_1 = \frac{3\pi}{8}\frac{m}{\mu}\frac{\Delta U}{U}\sqrt{k} \tag{4}$$

and the dimensionless traction is

$$J_4 = \frac{F_x}{\mu F_z} \tag{5}$$

This traction J_4 is a function of J_1 and k, as shown in figure 5. It may be observed from figure 5 that contacts of low aspect ratio have a superior performance in terms of traction at a given slip value.

Influence of Spin on Traction

For the combined action of slip and spin the resulting traction is given in figure 6. Dimensionless spin is defined as

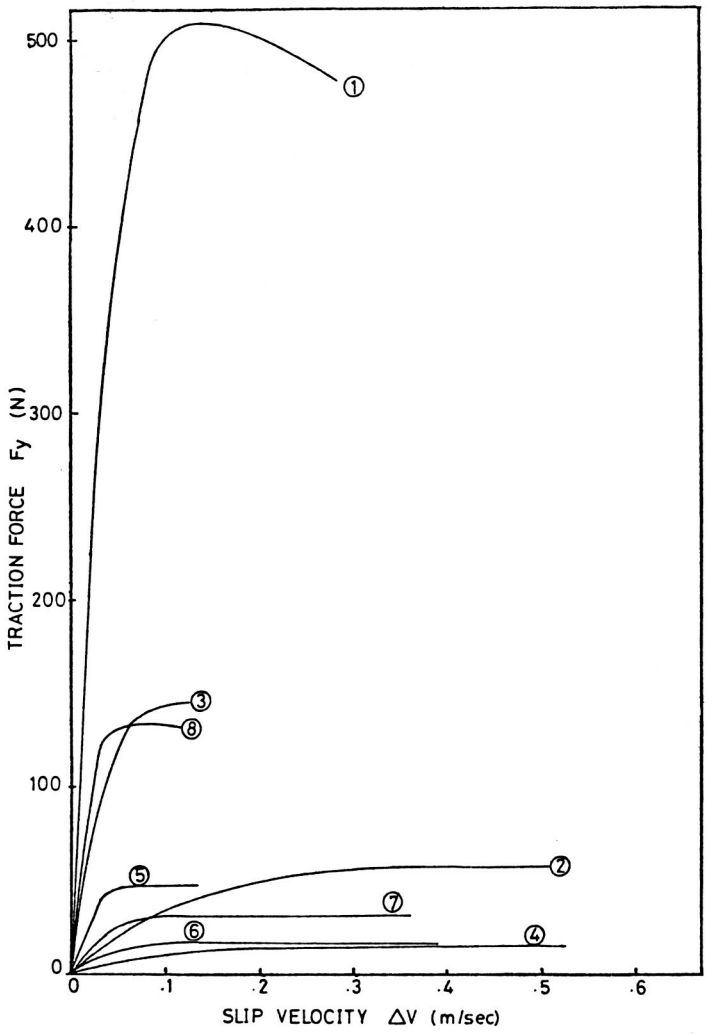

Fluid type	curve number	inlet temp	Hertz press.	speed U	aspect ratio	normal load
(-)	(-)	(°C)	(GPa)	(m/sec)	(-)	(N)
SANTO 50	1	32	1.45	20	5	5000
"	2	69	1.0	80	5	1500
"	3	29	1.9	20	1	1400
"	4	69	1.0	80	1	200
TDF-88	5	30	1.9	10	1	416
"	6	70	1.45	30	1	185
"	7	70	1.0	30	5	460
"	8	33	1.45	10	5	1400

Figure 3. - Typical traction curves obtained on two fluids at a range of speeds, aspect ratios, inlet temperatures, and contact pressures.

$$J_3 = \frac{3\pi}{8} \frac{m}{\mu} \frac{\omega\sqrt{ab}}{U} \sqrt{k} \tag{6}$$

No known analytical solution exists, and the results were obtained by digital integration. The influence of spin is to increase the slip, though this appears to be so only above a certain threshold value of spin. When the spin is sufficiently high, it is expected that elastic strain may be neglected and the rigid/plastic model may be used.

The resulting traction due to the shear of a rigid/plastic-like material in the contact is shown in figure 7. The independent parameters are the aspect ratio k and the speed pole location ϵ. The speed pole location parameter is identical to that used by Magi (ref. 14). It is related to the dimensionless parameters used in this analysis as follows:

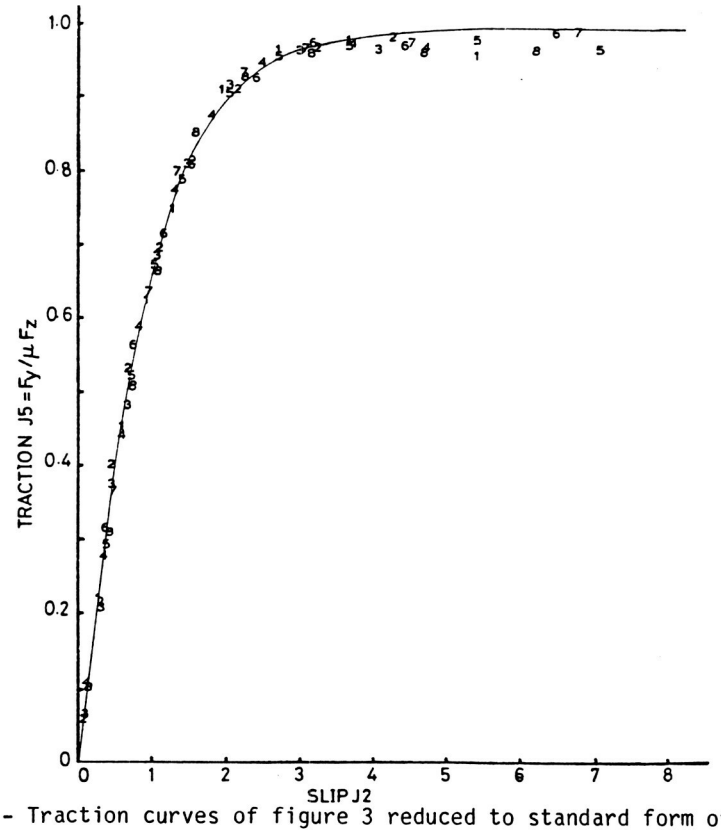

Figure 4. - Traction curves of figure 3 reduced to standard form of elastic/plastic curve.

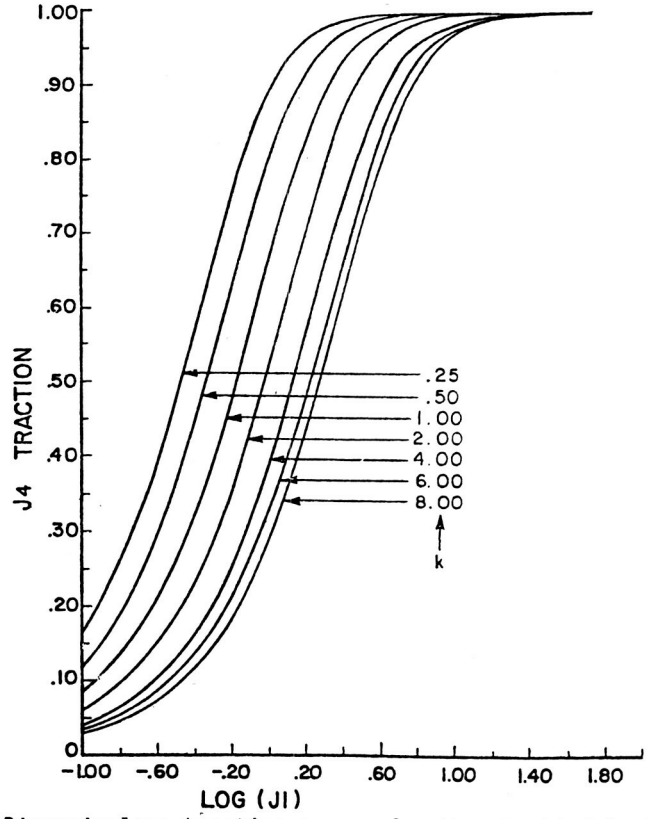

Figure 5. - Dimensionless traction curves for the elastic/plastic traction model at various ratios. These may be collapsed into one by dividing J_1 by $\sqrt{k}$.

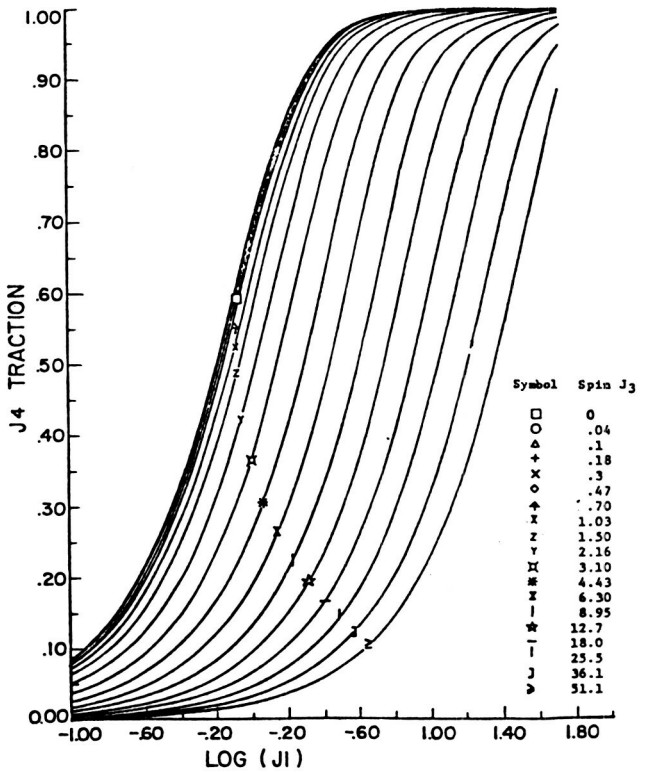

Figure 6. - Dimensionless traction curves for the elastic/plastic traction model under combinations of spin, J_3, and slip, J_1, for an aspect ratio of $\sqrt{k} = 1$.

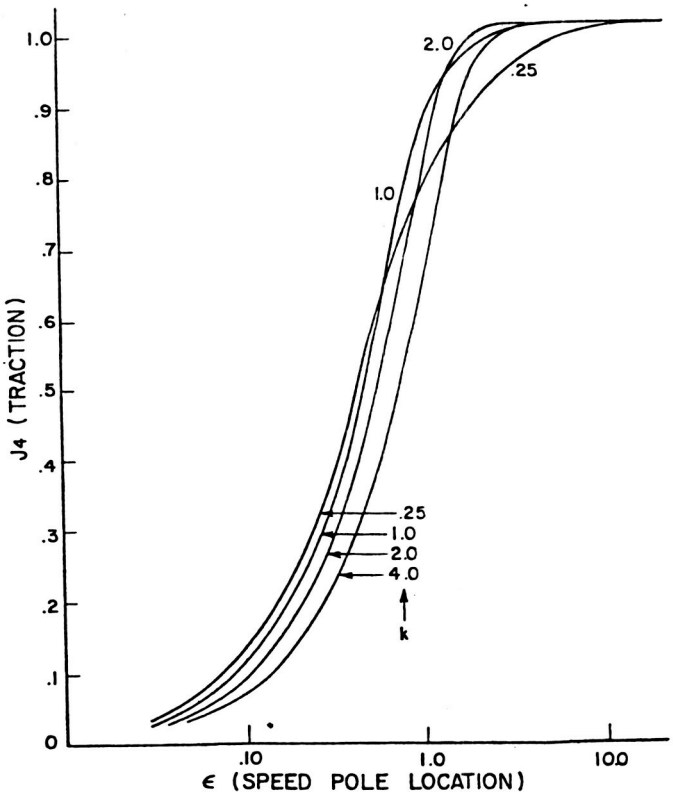

Figure 7. - Dimensionless traction curves for the rigid/plastic traction model at different speed pole locations. The speed pole location is given by $\epsilon = J_3/J_1$.

$$\epsilon = \frac{J_1}{J_3} = \frac{\Delta U}{\omega\sqrt{ab}} \tag{7}$$

Comparison with results obtained by Magi showed complete agreement. The results were obtained by numerical integration, and no known analytic expression exists for the traction in terms of the speed pole parameters. However, the curves shown in figure 7 do lend themselves to a simple empirical expression of the form:

$$J_4 = 1 - \exp[-(\epsilon k_1)^{k_2}] \tag{8}$$

This expression can also be written explicitly for ϵ. Coefficients k_1 and k_2 are given in table I for various aspect ratios. The largest error between the theoretical and predicted traction, according to equation (8), occurs in the low traction region and is less than 7 percent of the peak traction coefficient.

The traction curves and the influences of spin, as shown in figure 6, can be divided into three regions of influence. These regions are shown in figure 8 as a function of aspect ratio and dimensionless spin. The three regions represent:

(1) Traction predicted by neglecting spin and by using the elastic/plastic model
(2) Traction predicted by using the elastic/plastic model and by including spin
(3) Traction predicted by using the rigid/plastic model and by including spin.

It is in this latter region, where thermal effects become important, the methods outlined by Tevaarwerk (ref. 15) may have to be used to obtain more accurate traction predictions.

Influence of Side Slip on Traction

For the combined action of slip and side slip, the resulting traction J_4 for an elastic/plastic model are given by

$$J_4 = \frac{2}{3}\frac{J_1\psi}{S\sqrt{k}} \tag{9}$$

where

$$S = \frac{2}{3\sqrt{k}}\sqrt{(J_1^2 + J_2^2)}$$

$$J_2 = \frac{3\pi}{8}\frac{m}{\mu}\frac{\Delta V}{U}\sqrt{k}$$

and

$$\psi = \frac{1}{\pi}\left[2\tan^{-1} S + \frac{2S}{1+S^2}\right]$$

Figure 9 shows traction J_4 as a function of slip J_1 at various levels of J_2 for an aspect ratio of $k = 1$. The effect of side slip J_2 is to reduce the obtained traction in the working range.

When the imposed side slip becomes sufficiently large, the elastic effects may be neglected, and the traction can then be obtained by the rigid/plastic model:

$$J_4 = \frac{J_1}{\sqrt{J_1^2 + J_2^2}} \tag{10}$$

The reader might inquire as to the importance of being able to calculate the effect of side slip on traction. Side slip in traction drives results from misalinement of the axes of rotation of the principal shafts. Only very little misalinement is needed before 0.1 to 0.2 percent side slip is introduced. This can influence the longitudinal traction significantly, especially when little spin is present on the contact.

TABLE 1. – COEFFICIENTS FOR THE RIGID/PLASTIC TRACTION CURVE EXPRESSION

Aspect ratio, k	k_1	k_2
0.5	1.8	0.9
1.0	1.9	1.1
2.0	1.4	1.5
4.0	1.1	1.5
8.0	.8	1.5

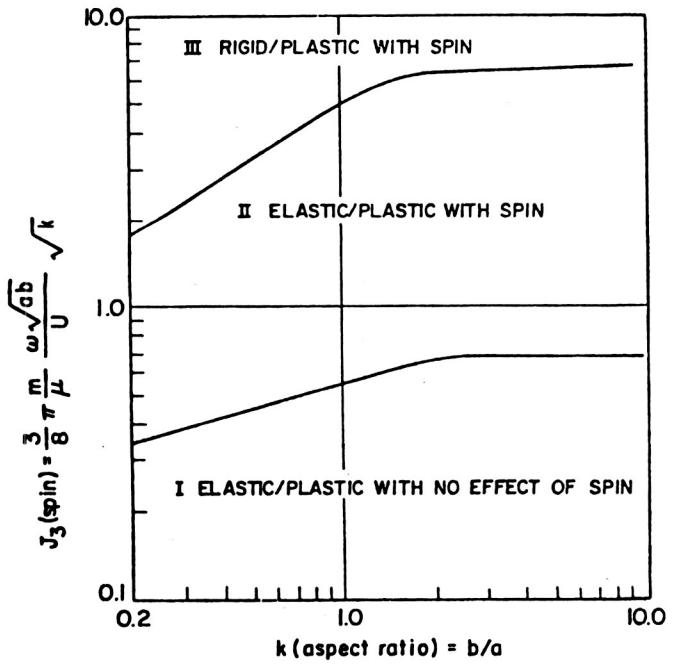

Figure 8. - Regions of influence of spin on the traction prediction of an elastic/plastic model. Dimensionless traction, J_4, is maintained at 0.75.

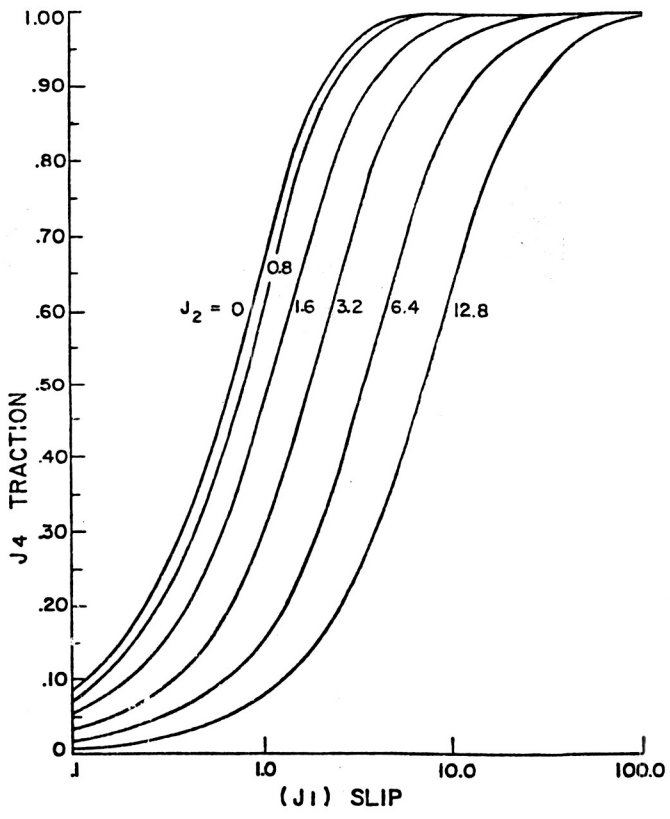

Figure 9. - Dimensionless traction curves predicted for combinations of slip, J_1, and side slip, J_2, using the elastic/plastic model.

Fluid Traction Data

Without the knowledge of the two fluid traction parameters, m and μ, the above models are not much use to the traction-drive designer. They do indicate traction trends when one or two parameters are varied, but no quantitative data can be obtained from them. To use the theory effectively one does need m and μ. These are related to fundamental fluid properties as we have seen before, but how these fundamental properties tie in with molecular structure of the fluid is not yet fully understood and often one resorts to experimentally available data for the particular fluid of interest.

To generate the experimental traction data for two fluids the Bearing, Gearing, and Transmission Section of NASA Lewis managed an extensive traction research under a Department of Energy program. This research was undertaken by Transmission Research, Inc. The main purpose of this research was to establish the traction parameters for two high-traction fluids at high speeds (10- to 80-m/sec surface velocity), at various contact aspect ratios ($k = 0.5$ to 5), at inlet temperatures of 30° to 70° C, and at contact pressures as encountered in traction drives. Also, the traction was measured under a variety of spin, side slip, and longitudinal slip combinations.

The traction data obtained from this investigation is reported by Tevaarwerk (ref. 18). The two important parameters for the traction curves were extracted and correlated with the various independent parameters that were imposed.

Traction Data Correlation

Examination of the traction parameters obtained by the above investigation revealed that there are certain trends when one of the external parameters, such as pressure, speed, inlet temperature or aspect ratio, is varied. The trends are

- Traction coefficient decreases with decreasing pressure.
- Traction coefficient decreases with increasing speed.
- Traction coefficient decreases with increasing temperature.
- Traction coefficient decreases with increasing aspect ratio.

Similar observations were found on the initial traction slope. By linearization of these trends the following equations may be written:

$$\mu \propto A_1 + A_2 P \qquad \mu \propto A_3 + A_4 U \qquad \mu \propto A_5 + \frac{A_6}{\theta} \qquad \mu \propto A_7 + A_8 k \tag{11}$$

These equations can be used directly for correlation purposes; however, to reduce the influence of weighting, because of the physical magnitude of certain of the variables, nondimensional variables should be used. These can be obtained quite easily by using transformations of the type

$$U' = \frac{U - \bar{U}}{\bar{U}} \qquad P' = \frac{P - \bar{P}}{\bar{P}} \qquad \theta' = \frac{\theta - \bar{\theta}}{\bar{\theta}} \qquad k' = \frac{k - \bar{k}}{\bar{k}} \tag{12}$$

where the prime indicates the transformed variable and the barred variable is the average magnitude. Because the trends are all equally likely for a given condition of speed, temperature, pressure, and aspect ratio, the following general equation may be expected:

$$\mu = (A_1 + A_2 P')(A_3 + A_4 U')\left(A_5 + \frac{A_6}{\theta'}\right)(A_7 + A_8 k') \tag{13}$$

Multiplication yields the following expression:

$$\mu = C_1 + C_2 k' + C_3 P' + C_4 P' k' + \frac{C_5}{\theta'} + C_6 \frac{k'}{\theta'} + C_7 \frac{P'}{\theta'} + C_8 k' \frac{P'}{\theta'} + C_9 U' + C_{10} U' k'$$
$$+ C_{11} U' P' + C_{12} U' P' k' + C_{13} \frac{U'}{\theta'} + C_{14} k' \frac{U'}{\theta'} + C_{15} P' \frac{U'}{\theta'} + C_{16} k' P' \frac{U'}{\theta'} \tag{14}$$

where the coefficient C_1 to C_{16} are directly related to the coefficients A_1 to A_8.

Initial Traction Slope

Equation (14) was also used on the initial traction slope data to obtain the coefficients C_1 to C_{16} by a least squares regression. The resulting regression coefficients are shown in appendix A for the two fluids tested. For these regression coefficients all the traction slopes for a given fluid were nondimensionalized by using equation (12). Before one can use the regression results to predict the initial traction slope, the variables need to be transformed according to this equation. This requires the knowledge of the average quantities of the variables and these are given in appendix A. Thus equation (14) can also be used to predict initial slope in using the appropriate coefficients C_1 to C_{16} given in appendix A.

Traction Coefficients

A similar analysis to the above could be done for the peak traction coefficient; however, it is also influenced by thermal effects due to spin. When spin is present, therefore, a further variation in the traction coefficient is possible. A similar treatment to the initial traction slope results gives the following expression for the traction coefficient:

$$\begin{aligned}\mu = {} & C_1 + C_2 Z' + C_3 k' + C_4 k' Z' + C_5 P' + C_6 P' Z' + C_7 P' k' + C_8 P' k' Z' + \frac{C_9}{\theta'} + C_{10}\frac{Z'}{\theta'} + C_{11}\frac{k'}{\theta'} \\ & + C_{12} k' \frac{Z'}{\theta'} + C_{13}\frac{P'}{\theta'} + C_{14} P' \frac{Z'}{\theta'} + C_{15} k' \frac{P'}{\theta'} + C_{16} k' P' \frac{Z'}{\theta'} + C_{17} U' + C_{18} U' Z' \\ & + C_{19} U' k' + C_{20} U' k' Z' + C_{21} U' P' + C_{22} U' P' Z' + C_{23} U' P' k' + C_{24} U' P' k' Z' \\ & + C_{25}\frac{U'}{\theta'} + C_{26} U' \frac{Z'}{\theta'} + C_{27} k' \frac{U'}{\theta'} + C_{28} U' k' \frac{Z'}{\theta'} + C_{29} P' \frac{U'}{\theta'} + C_{30} U' P' \frac{Z'}{\theta'} \\ & + C_{31} k' P' \frac{U'}{\theta'} + C_{32} U' k' P' \frac{Z'}{\theta'} \end{aligned} \tag{15}$$

where

$$Z = \frac{\omega\sqrt{ab}}{U}$$

and

$$Z' = \frac{Z - \overline{Z}}{\overline{Z}}$$

The regression coefficients for the traction coefficient of the two fluids are given in appendix A. They can be used to predict the traction coefficient whether spin is present or not.

It could be argued that a regression of the above type is not desirable because of the large number of coefficients involved. This is certainly true, and it is hoped that at some future time all the data can be reduced to two or three fundamental fluid parameters. However, such a model has not been sufficiently developed for inclusion here.

Example Traction Predictions

As an example of how the foregoing material may be used, let us take a look at some existing traction information and see how well the current methods will predict this traction. We will take some traction results as reported by Gaggermeier (ref. 19) and shown in figure 10. These data were

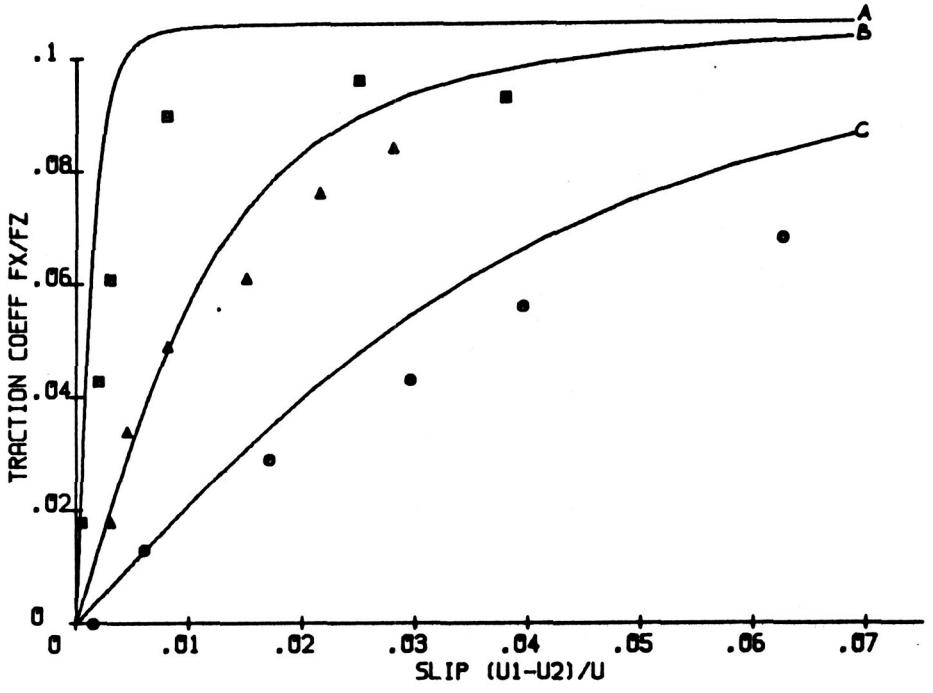

Figure 10. - Comparisons of measured and predicted traction under slip and side slip combinations. The following side slip was applied: ■ and curve A, 0 percent; ▲ and curve B, 1.57 percent; ● and curve C, 4.93 percent.

obtained on Santotrac 50 at a peak pressure of 1.854 GPa, an inlet temperature of 50° C, and a rolling speed of 8.4 m/sec. The aspect ratio for the contact was 1.5. The three sets of data points shown are for different degrees of side slip. These data, then, are a combination of side slip and longitudinal slip. The traction prediction based upon the elastic/plastic model as presented here is given by equation (9). To predict the actual traction, we need to know the initial traction slope and the peak traction coefficient for the particular fluid under the experimental conditions. These two parameters may be predicted by using the correlated data as reported here. We need to use equations (14) or (15) together with the coefficients as listed in appendix A. For Santotrac 50 at the particular conditions, as applicable to the experimental data, we get

$$m = 55.3$$

$$\mu = 0.106 \tag{16}$$

These two values can then be used in predicting the traction from equation (9). The predicted traction is shown in figure 10 as solid curves. It may be observed that the predicted values are somewhat higher than the experimental data. The most probable reason for this difference is the influence of thermal effects, which tend to reduce the traction at higher slip values. To get an improved prediction, methods as outlined in references 15 and 16 should be used.

Conclusion

In this paper it has been demonstrated how the traction performance of a typical drive can be

predicted from the basic knowledge of two fluid parameters, the initial traction slope, and the peak traction coefficient. These two parameters are given for two high-traction fluids as a function of inlet temperature, contact pressure, surface velocity, aspect ratio, and, in the case of the peak traction coefficient, the amount of spin on the contact. The traction behavior of the two fluids is very similar, with only minor differences. Thermal effects are not treated in this paper but can play a major part in the traction behavior of a contact. Current research indicates that a fairly simple thermal correction gives very good results. Also, very recent research by the author has indicated that the fundamental fluid properties of shear modulus and fluid shear strength can be represented by as few as three terms involving pressure and temperature only.

References

1. Clark, O. H.; Woods, W. W.; and White, J. R.: Lubrication at Extreme Pressure with Mineral Oil Films. J. Appl. Phys., vol. 22, no. 4, Apr. 1951, pp. 474-483.
2. Hewko, L. O.: Contact Traction and Creep of Lubricated Cylindrical Rolling Elements at Very High Surface Speeds. ASLE Trans., vol. 12, 1969, pp. 151-161.
3. Smith, F. W.: The Effect of Temperature in Concentrated Contact Lubrication. ASLE Trans., vol. 5, no. 1, Apr. 1962, pp. 142-148.
4. Smith, R. L.; Walowit, J. A.; and McGrew, J. M.: Elastohydrodynamic Traction Characteristics of 5P4E Polyphenyl Ether. J. Lubr. Technol., July 1973, pp. 353-362.
5. Johnson, K. L.; and Cameron, R.: Shear Behaviour of Elastohydrodynamic Oil Films at High Rolling Contact Pressures, Proc. Inst. Mech. Eng. (London), vol. 182, pt. I, no. 14, 1967, pp. 307-319.
6. Niemann, G.; and Stoessel, K.: Reibungszahlen bei elasto-hydrodynamisher Schmierung in Reibrad- und Zahnradgetrieben. Konstruktion, vol. 23, no. 7, 1971, pp. 245-260.
7. Johnson, K. L.; and Roberts, A. D.: Observations of Viscoelastic Behaviour of an Elastohydrodynamic Oil Film. Proc. Roy. Soc. (London), Ser. A, vol. 337, no. 1609, Mar. 19, 1974, pp. 217-242.
8. Johnson, K. L.; and Tevaarwerk, J. L.: Shear Behaviour of Elastohydrodynamic Oil Films. Proc. Roy. Soc. (London), Ser. A, vol. 356, no. 1685, Aug. 24, 1977, pp. 215-236.
9. Daniels, B. K.: Non-Newtonian Thermo-viscoelastic EHD Traction from Combined Slip and Spin. ASME Preprint 78-LC-2A-2, Oct. 1978.
10. Hirst, W., and Moore, A. J.: The Effect of Temperature on Traction in Elastohydrodynamic Lubrication. Phil. Trans. Roy. Soc. (London), Sept. 1980, vol. 298, no. 1438, pp. 183-208.
11. Alsaad, M.; Bair, S.; Sandorn, D. M.; and Winer, W. O.: Glass Transition in Lubricants: Its Relation to Elastohydrodynamic Lubrication. J. Lubr. Technol., vol. 100, July 1978, pp. 404-417.
12. Johnson, K. L.: Introductory Review of Lubricant Rheology and Traction. Proc. Leeds-Lyon Conf., Leeds, England, 1978, pp. 155-161.
13. Tevaarwerk, J. L.: Traction Drive Performance Prediction for the Johnson and Tevaarwerk Traction Model. NASA TP-1530, 1979.
14. Magi, Mart: On Efficiencies of Mechanical Coplanar Shaft Power Transmissions. Chalmers University of Technology, Gothenburg, Sweden, 1974.
15. Tevaarwerk, J. L.: A Simple Thermal Correction for Large Spin Traction Curves. J. Mech. Des., vol. 103, no. 2, April 1981, pp. 440-446.
16. Tevaarwerk, J. L.: Thermal Influence on the Traction Behaviour of an Elastic/Plastic Model. Proc. Leeds/Lyon Conf., Leeds, England, 1980.
17. Tevaarwerk, J. L.; and Johnson, K. L.: The Influence of Fluid Rheology on the Performance of Traction Drives. ASME J. Lubr. Technol., vol. 101, p. 266, 1979.
18. Tevaarwerk, J. L.: Traction Contact Performance Evaluation at High Speeds. NASA CR-165226, 1980.
19. Gaggermeier, H.: Untersuchungen zur Reibkraftuebertragung in Regel-Reibradgetrieben im Bereich elasto-hydrodynamischer Schmierung. Ph.D. Dissertation, University of Munich, 1977.

Appendix A

This appendix contains the regression coefficients for the traction data from the two fluids. The coefficients for slope are listed under column "m," and the coefficients for the traction coefficient are listed under "μ."

Coefficient	Santotrac 50			Sunoco TDF-88		
	μ eq. (14)	μ eq. (15)	m eq. (14)	μ eq. (14)	μ eq. (15)	m eq. (14)
$\overline{U}$	44.906	45.933	45.890	22.340	23.076	22.476
$\overline{P}$	1.356	1.331	1.369	1.449	1.408	1.424
$\overline{\theta}$	53.491	53.420	54.890	49.489	50.296	49.076
$\overline{K}$	3.340	3.321	2.753	2.239	2.441	2.262
$\overline{Z}$		5.786E-03			.639E-03	
C1	0.843E-01	0.745E-01	0.450E-02	0.877E-01	0.859E-01	0.452E-02
C2	-.685E-02	-.536E-02	-.719E-01	-.515E-02	-.582E-03	-.492E-01
C3	.434E-01	-.175E-02	.114E-02	.154E-01	-.480E-02	.649E-01
C4	.421E-01	-.219E-02	.109E-01	-.379E-02	.581E-03	-.102E-02
C5	-.960E-03	.204E-01	-.701E-01	-.676E-03	.162E-01	.202E-01
C6	.114E-02	-.208E-01	-.817E-01	-.428E-03	.211E-03	-.154E-01
C7	-.449E-03	.109E-01	.444E-00	.444E-03	-.601E-02	-.559E-00
C8	-.120E-02	-.258E-02	.805E-00	-.346E-02	-.542E-04	.609E-00
C9	-.197E-01	-.592E-03	-.755E-01	-.126E-01	-.102E-02	-.124E-02
C10	.299E-02	-.415E-03	-.577E-00	.356E-02	-.353E-03	.101E-02
C11	.350E-01	.705E-03	.124E-02	.141E-01	-.136E-03	.157E-02
C12	.664E-02	.957E-03	.115E-02	.764E-02	.401E-03	.270E-01
C13	.172E-02	.176E-02	-.921E-02	.167E-02	-.132E-02	-.639E-00
C14	-.317E-02	.305E-02	-.759E-01	.317E-03	-.848E-03	.558E-00
C15	-.285E-02	-.588E-02	.173E-00	-.851E-04	-.255E-02	.245E-01
C16	.956E-02	-.427E-02	.250E-01	.532E-02	.103E-02	-.196E-01
C17		-.162E-01			-.137E-01	
C18		-.273E-02			-.585E-03	
C19		-.534E-02			.344E-02	
C20		-.907E-03			.143E-02	
C21		.490E-01			.277E-02	
C22		.282E-01			-.382E-02	
C23		-.406E-01			.141E-01	
C24		-.588E-01			.701E-02	
C25		.324E-03			.177E-02	
C26		.790E-04			.104E-03	
C27		-.138E-04			-.162E-02	
C28		-.302E-03			-.723E-03	
C29		-.993E-02			-.850E-04	
C30		-.112E-01			.791E-03	
C31		.212E-01			.389E-03	
C32		.202E-01			-.291E-02	